

# An Uncharged Region within the N Terminus of the P2X<sub>6</sub> Receptor Inhibits Its Assembly and Exit from the Endoplasmic Reticulum<sup>§</sup>

Susan J. Ormond, Nelson P. Barrera, Omar S. Qureshi, Robert M. Henderson, J. Michael Edwardson, and Ruth D. Murrell-Lagnado

Department of Pharmacology, University of Cambridge, Cambridge, United Kingdom

Received October 27, 2005; accepted February 1, 2006

## ABSTRACT

ATP-gated P2X receptors are trimeric complexes formed by the homomeric or heteromeric assembly of seven different subunits. We have shown previously that, unlike all of the other P2X subunits, the P2X<sub>6</sub> subunit cannot form homomeric receptors and when expressed alone is retained in the endoplasmic reticulum (ER) in monomeric form (*J Biol Chem* **280**:107591–10765, 2005). However, other studies have shown that P2X<sub>6</sub> can form functional heteromeric receptors with P2X<sub>2</sub> and P2X<sub>4</sub> subunits. In this study, we used a combination of immunocytochemistry, surface biotinylation, and atomic force microscopy to investigate the assembly and trafficking of the P2X<sub>6</sub> subunit, both alone and as part of a heteromer. We show that as a heteromer, it exits the ER and is either stably expressed at the cell surface or constitutively internalized, depending on its

partner. Through the use of targeted mutation, we demonstrate that an uncharged region at the N terminus of P2X<sub>6</sub> exerts an inhibitory effect on its assembly and export from the ER. When this region is removed, or when charge is added to it, P2X<sub>6</sub> forms homotrimeric assemblies, undergoes complex glycosylation and is delivered to the plasma membrane, albeit less efficiently than the P2X<sub>2</sub> receptor. The N-terminal mutants were, however, nonfunctional. Substituting the uncharged 14-amino acid N-terminal region for the equivalent region of P2X<sub>2</sub> increased ER retention but was not sufficient to prevent the formation of functional homomeric receptors. We propose that the N terminus of the P2X<sub>6</sub> subunit contributes to a mechanism that prevents the inappropriate export and plasma membrane expression of nonfunctional P2X receptors.

Ionotropic receptors have been grouped into three major structural classes, with purinergic P2X receptors forming a class distinct from the cysteine loop and glutamate receptor families (North, 1996). P2X subunits (P2X<sub>1–7</sub>) have two transmembrane regions, a large extracellular loop, and intracellular N and C termini (Torres et al., 1998), and they assemble to form homo- and heterotrimeric complexes (Soto et al., 1996; Nicke et al., 1998; Torres et al., 1999). Assembly of ionotropic receptors from their constituent subunits takes place in the endoplasmic reticulum (ER) (Deutsch, 2003). This key step in receptor formation is monitored by quality control systems within the ER that prevent misassembled receptors reaching the plasma membrane. These mecha-

nisms include retention by ER chaperones and recognition of short amino acid sequences, known as retention or export motifs, that can, respectively, prevent or promote the exit of proteins from the ER (Ellgaard and Helenius, 2003). Of the seven P2X subtypes, only P2X<sub>6</sub> is unable to form functional homomeric receptors (Torres et al., 1999a), and it is retained within the ER (Bobanovic et al., 2002). Evidence from biochemical analysis and atomic force microscopy (AFM) imaging of these receptors indicates a failure to form stable trimers (Aschrafi et al., 2004; Barrera et al., 2005).

Despite not forming homomeric receptors, P2X<sub>6</sub> readily forms heteromers with P2X<sub>2</sub> and P2X<sub>4</sub>, producing receptors with properties different from those of the parent receptors (King et al., 2000). For example, the calcium permeability of the P2X<sub>2/6</sub> heteromer is significantly greater than that of the P2X<sub>2</sub> homomers (Egan and Khakh, 2004). This could have important implications in synaptic transmission, because these two subunits have overlapping pre- and postsynaptic distributions (Vulchanova et al., 1996; Loesch and Burn-

This work was supported by the Biotechnology and Biological Sciences Research Council.

Article, publication date, and citation information can be found at <http://molpharm.aspetjournals.org>.  
doi:10.1124/mol.105.020404.

<sup>§</sup> The online version of this article (available at <http://molpharm.aspetjournals.org>) contains supplemental material.

**ABBREVIATIONS:** ER, endoplasmic reticulum; AFM, atomic force microscopy; DSS, disuccinimidyl suberate; EGFP, enhanced green fluorescent protein; Endo H, endoglycosidase H; FITC, fluorescein isothiocyanate; HA, hemagglutinin; HEK, human embryonic kidney; NRK, normal rat kidney; PBS, phosphate-buffered saline; PAGE, polyacrylamide gel electrophoresis; CHAPS, 3-[(3-cholamidopropyl)dimethylammonio]propanesulfonate.

stock, 2001; Rubio and Soto, 2001). In fact, P2X<sub>2</sub>, P2X<sub>4</sub>, and P2X<sub>6</sub> subunits are reported to be coexpressed in many areas of the central nervous system, including olfactory bulb neurons, Purkinje cells of the cerebral cortex, CA1 cells of the hippocampus, and ventral horn motoneurons (Collo et al., 1996; Seguela et al., 1996; Soto et al., 1996; Le et al., 1998; Kukley et al., 2001). Outside the central nervous system, P2X<sub>6</sub> is again coexpressed with P2X<sub>4</sub> in vascular endothelial cells and kidney tubule epithelial cells (Glass et al., 2002; Turner et al., 2003).

The molecular basis for the unique inability of the P2X<sub>6</sub> subunit to assemble correctly when expressed alone and for its retention in the ER is unknown. Previous studies have produced conflicting results. Blue native polyacrylamide gel electrophoresis (PAGE) analysis of P2X<sub>6</sub> expressed in *Xenopus laevis* oocytes showed the formation of large aggregates and homotetrameric assemblies (Aschrafi et al., 2004). Furthermore, there was no expression of P2X<sub>6</sub> protein at the plasma membrane. AFM imaging of P2X<sub>6</sub> purified from transfected tsA 201 cells showed particles of molecular volume corresponding to monomers, whereas P2X<sub>2</sub> receptors produced particles with the molecular volume expected of trimers (Barrera et al., 2005). Jones et al. (2004) showed that approximately 5% of P2X<sub>6</sub>-transfected human embryonic kidney (HEK) 293 cells produced functional receptors. Western blot analysis showed that P2X<sub>6</sub> protein from ATP-responsive cells was more extensively glycosylated, with a molecular mass of 70 kDa, compared with 60 kDa for nonresponsive cells. Collo et al. (1996) also reported the production of functional recombinant P2X<sub>6</sub> receptors, although with different pharmacological and kinetic properties from those reported by Jones et al. (2004).

In this study, we showed, using biochemical and confocal imaging methods, that the level of plasma membrane expression of P2X<sub>6</sub> in normal rat kidney (NRK) cells is very low and that the protein is retained in the ER in its core glycosylated state. When coexpressed with P2X<sub>2</sub> or P2X<sub>4</sub> subunits, P2X<sub>6</sub> showed only a very modest increase in molecular mass (1–2 kDa), acquired endoglycosidase H (Endo H) resistance, and was expressed at the plasma membrane. The second transmembrane region has been identified as a critical determinant of P2X subunit coassembly (Torres et al., 1999b). In this study, we identified an uncharged 14-amino acid region within the N terminus of P2X<sub>6</sub> that is not shared by other members of this family and which acts as a determinant of P2X<sub>6</sub> assembly and trafficking. Deletion of this region or the introduction of either positive or negative charge facilitated the homomeric assembly of P2X<sub>6</sub> and its delivery to the plasma membrane. The fusion of this region to the N terminus of the P2X<sub>2</sub> subunit enhanced the ER retention of the chimeric receptor. The P2X<sub>6</sub> N-terminal mutants that did traffic to the surface did not respond to extracellular ATP, suggesting that this N-terminal-dependent mechanism contributes to preventing the inappropriate export and plasma membrane expression of nonfunctional P2X receptors.

## Materials and Methods

**DNA Constructs.** The following rat P2X<sub>6</sub> receptor cDNAs were used: wild-type P2X<sub>6</sub> subunit with either a hemagglutinin (HA) tag or a His<sub>6</sub> tag at the C terminus; wild-type P2X<sub>6</sub> with a FLAG (DYKDDDDK) tag in the extracellular loop in place of residues Val80

to Glu84 and including Lys85; mutants of FLAG-tagged P2X<sub>6</sub> in which either the N-terminal 14 residues had been deleted (N-14) or residues Ser3 and Ser11 had been mutated to aspartic acid (S2D), alanine (S2A), or lysine (S2K); the same four mutants without the FLAG tag but bearing a C-terminal HA tag; and the S2K mutant bearing a C-terminal His<sub>6</sub> tag. All of these sequences were subcloned into the pEGFP vector so that the enhanced green fluorescent protein (EGFP) sequence was excised. Other constructs used were the following: pEGFP; wild-type rat P2X<sub>2</sub>; P2X<sub>2</sub> in which the first half of the P2X<sub>2</sub> N terminus was substituted with the uncharged N-terminal region of the P2X<sub>6</sub>, known as (6N14)P2X<sub>2</sub>; wild-type P2X<sub>4</sub>; P2X<sub>4</sub> tagged at its C terminus with EGFP and DsRed-ER (Clontech, Mountain View, CA).

**Cell Culture and Transient Transfection.** NRK cells and tsA 201 cells (a subclone of HEK 293 cells stably expressing the SV40 large T-antigen) were maintained in Dulbecco's modified Eagle's medium containing 10% fetal bovine serum, 2 mM glutamine, 100 U/ml penicillin, and 100 µg/ml streptomycin in a humidified incubator at 37°C and in 95% air/5% CO<sub>2</sub>. Transient transfections of NRK cells were carried out using Lipofectamine (Invitrogen, Carlsbad, CA), according to the manufacturer's instructions. For transfection of one 12-well plate, 12 µg of plasmid DNA was used. Transient transfections of tsA 201 cells with P2X<sub>6</sub> receptor DNA were carried out using the CalPhos mammalian transfection kit (Clontech) according to the manufacturer's instructions. For transfection of one 162-cm<sup>2</sup> culture flask, 30 µg of plasmid DNA was used. After transfection, cells were incubated for 24 to 48 h at 37°C to allow expression of the P2X receptors.

**Live-Labeling Immunofluorescence Protocols.** The basic protocol for live labeling was as follows: cells were incubated with anti-FLAG primary antibody diluted in Dulbecco's modified Eagle's medium for 30 min at 37°C. Cells were then washed five times and fixed in paraformaldehyde. To detect FLAG-labeled receptors at the surface, fixed nonpermeabilized cells were stained with an anti-mouse Cy3-conjugated secondary for 2 h at room temperature. Cells were then washed five times in phosphate-buffered saline (PBS) and permeabilized with 0.1% Triton X-100. To visualize intracellular receptors, the cells were incubated again with anti-FLAG primary antibody for 1 h at room temperature, followed by incubation with an anti-mouse fluorescein isothiocyanate (FITC)-conjugated secondary for 2 h.

**Image Analysis.** Fluorescence was visualized using a Zeiss Axiovert LSM510 confocal microscope using 63× oil immersion objective (Carl Zeiss Inc., Thornwood, NY). For FITC-Cy3 anti-FLAG double labeling, FITC and Cy3 were excited at 7 and 60% of 488 and 543 laser power, respectively. For individual experiments, images for all conditions were analyzed using identical acquisition parameters. Tagged-image file format images were imported into NIH Image software (ver. 1.62; <http://rsb.info.nih.gov/ni-image/>), and the cells outlined and mean pixel values for each channel were obtained. The images were selected so that the confocal plane was focused on the middle of the cell to exclude the signal from the top and the bottom of the cell. Pixel values were on an 8-bit scale (2<sup>8</sup> = 256; 0–255). Experiments were repeated at least twice, and each time, data were analyzed from at least 25 cells from two separate coverslips. Within each experiment the data were normalized to control cells. The *n* value given refers to the number of cells analyzed. All data are means ± S.E.M. Histograms and plots were constructed using Igor PRO 3.14 software (WaveMetrics, Lake Oswego, OR).

**Antibodies and Reagents.** The following primary antibodies were used: mouse monoclonal anti-FLAG M2 (2 µg/ml; Sigma, St. Louis, MO); rabbit polyclonal anti-P2X<sub>4</sub> subunit (6 µg/ml; Alomone Labs, Jerusalem, Israel), and anti-P2X<sub>2</sub> subunit (0.6 µg/ml; Alomone). FITC- and Cy3-conjugated goat anti-mouse or anti-rabbit antibodies (1:200) were used as secondary antibodies (Jackson ImmunoResearch Laboratories Inc., West Grove, PA). Unless otherwise stated, all other reagents were obtained from Sigma or Invitrogen.

**Deglycosylation of Proteins.** NRK cells, plated in six-well plates, were used 24 to 48 h after transfection. The cells were washed twice with PBS and collected directly into lysis buffer (100  $\mu$ l; 50 mM Tris-Cl, pH 8.0, 150 mM NaCl, 0.1% SDS, 1% Nonidet P-40, and 0.5% sodium deoxycholate). The cell lysate was sonicated and then left on ice for 30 min. Samples were then cleared by spinning in a cooled centrifuge at 14,000 rpm for 15 min. Proteins were denatured and treated with either *N*-glycosidase F (Roche, Indianapolis, IN), to remove all *N*-glycans, or Endo H (New England Biolabs, Beverly, MA), to remove "high-mannose" *N*-glycans, according to the manufacturer's instructions. Proteins were analyzed by SDS-PAGE and immunoblotting. The P2X<sub>2</sub> receptor was detected using a rabbit polyclonal anti-receptor antibody (1:500; Alomone Laboratories). The P2X<sub>6</sub> receptor (tagged at its C terminus with an HA epitope) was detected using a mouse monoclonal anti-HA antibody (1:500; Covance Research Products, Princeton, NJ). Immunoreactive bands were visualized using appropriate horseradish peroxidase-conjugated secondary antibodies (Perbio Science UK Ltd., Cramlington, Northumberland, UK; or Bio-Rad, Hercules, CA) followed by enhanced chemiluminescence.

**Biotinylation.** Cells were washed once with ice-cold PBS and incubated with 1 ml of sulfo-succinimidyl 2-(biotinamido)-ethyl-1,3'-dithiopropionate (Pierce, Rockford, IL) solution (freshly prepared on day of use; 1 mg/ml in PBS) for 20 min. Excess biotin was quenched by washing the cells once with PBS containing 50 mM glycine and twice with PBS. Cells were solubilized with lysis buffer and incubated on ice for 30 min, after which time they were sonicated and cleared by centrifugation. A portion of the supernatant was incubated with immobilized NeutrAvidin biotin binding protein beads (Pierce) on a rotating rack for 2 h at 4°C to precipitate biotinylated proteins. The rest of the supernatant was kept to assess total protein in each sample. After incubation, beads containing precipitated biotinylated proteins were spun for 1 min at 10,000 rpm at a temperature of 4°C. The supernatant was removed, and the beads were washed with lysis buffer. This was repeated three times, and the protein was eluted from the beads by incubation in 20  $\mu$ l of Laemmli buffer. Proteins were separated by SDS-PAGE and detected by immunoblotting as described above.

**Receptor Cross-Linking in Crude Detergent Extracts of Transfected Cells.** Transfected NRK cells, growing in six-well plates, were washed twice with phosphate-buffered saline (150 mM NaCl and 10 mM sodium phosphate, pH 7.4) and collected directly into lysis buffer (PBS containing 1% Triton X-100) and a protease inhibitor mixture (Roche). The cell lysate was left on ice for 30 min followed by sonication and clearing by centrifugation. The supernatant was then incubated either with or without disuccinimidyl suberate (DSS; Pierce and Warriner UK Ltd., Chester, UK; 4 mM) for 30 min at room temperature. Reactions were quenched by the addition of Tris-HCl, pH 7.5 (final concentration, 50 mM; 15 min at room temperature) and terminated by the addition of SDS-PAGE sample buffer. Proteins were separated by SDS-PAGE and detected by immunoblotting.

**Electrophysiological Recordings.** Standard whole-cell recordings were performed at room temperature using an Axopatch 200A amplifier (Axon Instruments, Sunnyvale, CA). Patch pipettes (3–8 M $\Omega$ ) were pulled from thick-walled borosilicate glass (GC150F-10; Harvard Apparatus, Holliston, MA) and filled with solution containing 125 mM potassium gluconate, 1 mM MgCl<sub>2</sub>, and 10 mM HEPES, pH 7.3. The extracellular solution was composed of 140 mM NaCl, 5 mM KCl, 2 mM CaCl<sub>2</sub>, 1 mM MgCl<sub>2</sub>, 10 mM D-glucose, and 10 mM HEPES, pH 7.3. ATP-evoked responses were measured at –60 mV.

Whole-cell currents were low-pass-filtered at 2 kHz and digitized at 10 kHz. ATP was applied locally using a Picospritzer II (Parker Instrumentation, Cleveland, OH). To ensure the delivery of drug, 0.05% (w/v) fast green was used (local applications of 1% fast green evoked no response). To visualize cells expressing P2X receptors, cells were cotransfected with green fluorescent protein (0.5  $\mu$ g of pEGFP-N1 vector included in precipitate) and were observed under

a microscope with an epifluorescence attachment (Nikon, Tokyo, Japan). Untransfected cells and cells expressing green fluorescent protein alone were found to have no inward current in response to application of ATP. Acquisition was performed using HEKA Pulse 8.30 (HEKA, Lambrecht/Pfalz, Germany), and data were subsequently analyzed using Igor PRO 3.16.

**Solubilization and Purification of His<sub>6</sub>-Tagged P2X<sub>6</sub> Receptors.** The solubilization/purification procedure was identical with that described previously and relied on the binding of the receptor via its His<sub>6</sub> tag to Ni<sup>2+</sup>-agarose (Barrera et al., 2005). In brief, a crude membrane fraction prepared from transfected tsA 201 cells was solubilized in 1% (w/v) CHAPS, and the solubilized material was incubated with Ni<sup>2+</sup>-agarose beads (Probond; Invitrogen). The beads were washed extensively, and bound protein was eluted with increasing concentrations of imidazole. Samples were analyzed by SDS-PAGE, and protein was detected by immunoblotting. The receptor was detected using mouse monoclonal antibodies against the His<sub>6</sub> tag (Invitrogen; 1:500).

**AFM Imaging of Receptors and Receptor-Antibody Complexes.** Receptors were imaged either alone or after incubation for 14 h at 4°C with a 1:2 M ratio (approximately 0.2 nM receptor concentration) of anti-His<sub>6</sub> IgG (Research Diagnostics Inc., Flanders, NJ). Proteins were diluted in wash buffer (above) to a final concentration of 0.04 nM, and 45  $\mu$ l of the sample was allowed to adsorb to freshly cleaved, poly(L-lysine)-coated mica coverslips (Sigma). After a 10-min incubation, the sample was washed with MilliQ-water and dried under nitrogen. Imaging was performed with a Multimode atomic force microscope (Digital Instruments Corporation, Gujarat, India). Samples were imaged in air. Experiments were carried out in tapping mode, and the silicon cantilevers used had a drive frequency of ~300 kHz and a specified spring constant of 40 N/m (MikroMasch, Wilsonville, OR). The applied imaging force was kept as low as possible (target amplitude, ~1.6–1.8 V; amplitude setpoint, ~1.3–1.5 V).

The molecular volumes of the protein particles were determined from particle dimensions based on AFM images. After adsorption of the receptors onto the mica support the particles adopt the shape of a spherical cap. The heights and half-height radii were measured from multiple cross-sections of the same particle, and the molecular volume was calculated using the equation  $V_m = (\pi h/6)(3r^2 + h^2)$ , where  $h$  is the particle height and  $r$  is the radius (Schneider et al., 1998). Molecular volume based on molecular mass was calculated using the equation  $V_c = (M_0/N_0)(V_1 + dV_2)$ , where  $M_0$  is the molecular mass,  $N_0$  is Avogadro's number,  $V_1$  and  $V_2$  are the partial specific volumes of particle and water, respectively, and  $d$  is the extent of protein hydration (Schneider et al., 1998). Because the receptors are glycoproteins, the volume contributions of core protein and attached oligosaccharides were calculated separately, using previously reported values of partial specific volumes for protein (0.74 cm<sup>3</sup>/g) and carbohydrate (0.61 cm<sup>3</sup>/g) (Durchschlag and Zipper, 1997). It has been shown (Schneider et al., 1998) that there are no significant differences in molecular volumes determined by imaging under fluid and in air (as in this study). Hence, for the extent of protein hydration, we used the value of 0.4 g of water/g of protein reported for a typical globular protein (human serum albumin) in solution (Grant, 1957).

When receptors were imaged after incubation with the various antibodies, note was taken of whether the receptors were untagged or tagged with one, two, or three antibodies. The results obtained were expressed as a percentage of the total number of particles for each sample. Zoomed images of receptors with two antibodies bound were inspected, and the angle separating the two antibodies was measured. The distribution of angles was analyzed, and the sample means were calculated.

## Results

**The Formation of Heteromers Enables the P2X<sub>6</sub> Subunit to Exit the ER.** We have shown that the P2X<sub>6</sub> receptor



subunit, expressed individually in HEK 293 cells, colocalizes with an ER reporter protein, calreticulin, but when coexpressed with P2X<sub>4</sub>, it colocalizes with a marker for early endosomes, EEA1 (Bobanovic et al., 2002). Likewise, in NRK cells, P2X<sub>6</sub> receptor subunits colocalized extensively with DsRed-ER (Fig. 1A) and did not produce functional ATP-gated ion channels, as determined by patch-clamp measurements (data not shown). To investigate the trafficking of P2X<sub>6</sub> along the secretory pathway in more detail, we compared the effects of *N*-glycosidase F and Endo H on the glycosylation status of P2X<sub>6</sub> expressed either alone or together with other members of the P2X receptor family. *N*-

glycosidase F can digest both high mannose sugars of the type found in the ER and mannose-trimmed, complex sugars generated in the Golgi, whereas Endo H can cleave high mannose sugars but is inactive against complex sugars (Maley et al., 1989). The P2X<sub>6</sub> subunit expressed alone migrated as a band at 52 kDa (Fig. 1B), and this collapsed to 45 kDa after treatment with either Endo H or *N*-glycosidase F (Fig. 1C), indicating that no complex glycosylation of P2X<sub>6</sub> had taken place. When the P2X<sub>6</sub> subunit was coexpressed with either the P2X<sub>2</sub> or the P2X<sub>4</sub> subunit, there was a small increase (1–2 kDa) in its molecular mass, and a new band appeared in the Endo H-treated samples, indicating that the protein had undergone partial complex glycosylation in the Golgi complex (Fig. 1, B and C).

Delivery of P2X<sub>6</sub> to the plasma membrane of transfected NRK cells was assayed by biotinylating surface proteins and immunoblotting for P2X<sub>6</sub> (Fig. 1D). When expressed alone, surface delivery as a proportion of total P2X<sub>6</sub> was very low, but it increased in the presence of either P2X<sub>2</sub> or P2X<sub>4</sub> subunits. With P2X<sub>4</sub>, biotinylated receptors containing P2X<sub>6</sub> subunits became internalized, and the biotin group was protected from cleavage by extracellularly applied glutathione, whereas internalization of P2X<sub>6</sub> in the presence of P2X<sub>2</sub> was less extensive (Fig. 1E). Surface expression of the P2X<sub>6</sub> subunit was also measured by immunofluorescence. An extracellular FLAG epitope was introduced just beyond TM1 to enable surface receptors to be labeled with an extracellular antibody. Similar FLAG and AU5-tagged P2X<sub>2</sub> and P2X<sub>4</sub> constructs were generated previously, and the insertion of the epitopes was shown not to disrupt receptor trafficking or function (Bobanovic et al., 2002). P2X<sub>6</sub>-FLAG was expressed either alone or with P2X<sub>2</sub> or P2X<sub>4</sub>, and live cells were incubated with anti-FLAG antibody at 37°C for 30 min. This procedure should label receptors delivered to the surface during this period even if they were subsequently retrieved. Surface versus intracellular immunofluorescence intensities were compared (Fig. 1F). In the presence of either P2X<sub>2</sub> or P2X<sub>4</sub>, there was an increase of approximately 6-fold in surface immunolabeling given by the P2X<sub>6</sub> subunit, with no significant change ( $P = 0.22$  and  $0.57$ ) in intracellular levels (Fig. 1G). Figure 1F, right, shows the total P2X<sub>2</sub> and P2X<sub>4</sub> immunolabeling in permeabilized cells.

**The Uncharged N-Terminal Region of the P2X<sub>6</sub> Subunit Promotes ER Retention.** We showed previously that P2X<sub>6</sub> does not form stable homotrimers (Barrera et al., 2005). It should, therefore, be recognized by the ER quality control machinery and retained. Retention is usually mediated via exposed hydrophobic segments or short motifs that are buried in the correctly assembled complex. The P2X<sub>6</sub> C terminus is short, does not contain a hydrophobic sequence of amino acids or a recognized ER retention motif, and does not confer ER retention when fused to the C terminus of the reporter protein CD8 (results not shown). The N terminus, however, has a stretch of 14 uncharged amino acids immediately after the first methionine, which is not conserved among the other P2X subtypes (Fig. 2A). To test its involvement in the trafficking and assembly of P2X<sub>6</sub>, a deletion construct lacking these 14 residues (N-14) was generated. Surface biotinylation revealed that, compared with wild-type P2X<sub>6</sub>, this deletion mutant had increased surface expression, although overall expression levels were not significantly different from wild type (Fig. 2B). There was also an Endo H-resistant

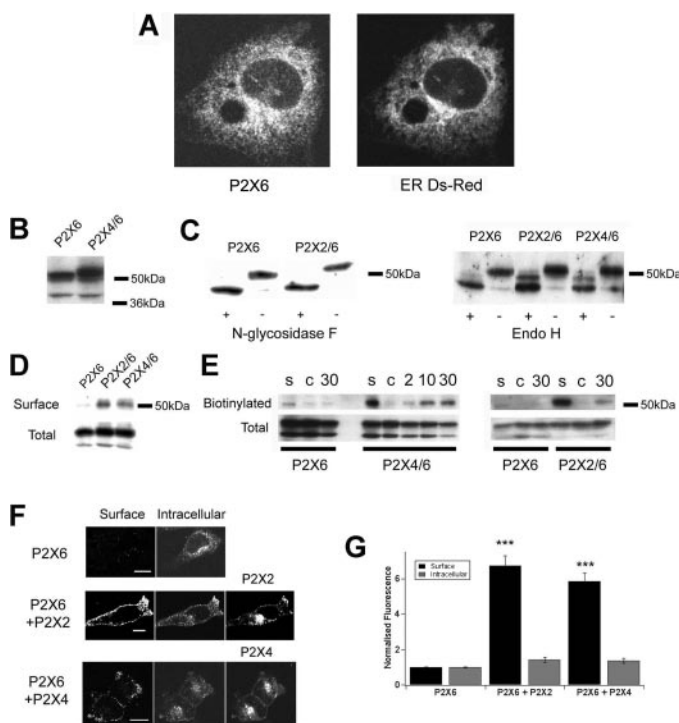


**Fig. 1.** Heteromerization of P2X<sub>6</sub> subunits with either P2X<sub>2</sub> or P2X<sub>4</sub> subunits alters its trafficking. **A**, confocal images show the ER localization of P2X<sub>6</sub> expressed in an NRK cell. The P2X<sub>6</sub> subunit was tagged with an HA epitope and stained with an anti-HA antibody followed by an FITC-conjugated secondary antibody. Ds-Red ER (Clontech) was coexpressed with P2X<sub>6</sub>. Scale bar, 10  $\mu$ m. **B** to **E**, SDS-PAGE and immunoblot analysis of crude detergent extracts of transfected NRK cells. **B**, extracts containing P2X<sub>6</sub> subunit either expressed alone or with P2X<sub>4</sub> were blotted for total P2X<sub>6</sub> protein to compare band sizes. **C**, extracts containing P2X<sub>6</sub> subunit either alone or with P2X<sub>2</sub> or P2X<sub>4</sub> were treated with *N*-glycosidase F or endoglycosidase H. **D** and **E**, intact transfected cells were incubated with biotin (1 mg/ml) for 20 min at 4°C to label surface proteins. **D**, cells were solubilized after biotinylation, and surface proteins were precipitated with streptavidin beads. Surface expression of P2X<sub>6</sub> increased in the presence of P2X<sub>2</sub> and P2X<sub>4</sub>, although totals show equivalent protein levels. **E**, surface proteins were biotinylated as before (lane s), and then cells were returned to 37°C for the indicated time before surface biotin was stripped by incubation in glutathione. Lane c represents cells that remained at 4°C throughout to measure the efficiency of cleavage. In all blots, P2X<sub>6</sub> subunit was detected with an anti-HA primary antibody followed by horseradish peroxidase-conjugated anti-mouse secondary antibody. **F**, confocal images of NRK cells expressing FLAG-tagged P2X<sub>6</sub> subunit alone or with either P2X<sub>2</sub> or P2X<sub>4</sub>. Cells were incubated before and after permeabilization with FLAG antibody followed by Cy3- and FITC-labeled secondary antibodies to detect surface and intracellular fluorescence, respectively. P2X<sub>2</sub> and P2X<sub>4</sub> were detected with anti-P2X<sub>2</sub> and anti-P2X<sub>4</sub> polyclonal antibodies after permeabilization, followed by a Cy5-conjugated secondary antibody. **G**, bar chart showing normalized surface/intracellular fluorescence for a number of cells ( $n = 55$ – $58$  cells for each condition).

fraction, indicating complex glycosylation and hence transport through the Golgi complex (Fig. 2C). Immunofluorescence analysis confirmed the delivery of the N-14 mutant to the cell surface (Fig. 2, D and E).

**ER Retention Is Correlated with Hydrophobicity at Positions 3 and 11.** Next, we tested the effect of introducing charge into the N-terminal region of the P2X<sub>6</sub> subunit to reduce its hydrophobicity. There are serine residues at positions 3 and 11 (Fig. 3A). Substitution of aspartates (S2D mutant) increased surface expression by approximately 3-fold, whereas substituting alanines (S2A mutant) produced a small but significant decrease, indicating that removal of the serines per se does not promote ER export (Fig. 3, B–D). Positively charged lysines (S2K mutant) produced the greatest increase in surface expression (approximately 4-fold), similar to that caused by the N-terminal deletion. The serine mutations in P2X<sub>6</sub> did not seem to alter the assembly or trafficking of the P2X<sub>4/6</sub> heteromers; when coexpressed with P2X<sub>4</sub>, the mutant P2X<sub>6</sub> subunits colocalized with P2X<sub>4</sub> in vesicular structures characteristic of endolysosomal compartments (Supplementary Fig. S1), as shown previously for wild-type P2X<sub>4</sub> homomeric and P2X<sub>4/6</sub> heteromeric receptors (Bobanovic et al., 2002). This result is consistent with our previous finding that the P2X<sub>4</sub> subunit plays a dominant role in determining the trafficking of the heteromeric receptor (Bobanovic et al., 2002).

**The P2X<sub>6</sub> S2K Mutant Forms Homotrimers.** The introduction of charged residues at positions 3 and 11 within the P2X<sub>6</sub> N terminus could either enable incorrectly assembled subunits to escape the ER quality control machinery or promote the formation of homotrimers. To distinguish between these two possibilities, we isolated wild-type and S2K mutant P2X<sub>6</sub> receptors from transfected tsA 201 cells and analyzed them by AFM. The wild-type receptor appeared as a relatively homogenous spread of particles (Fig. 4A, left); in contrast,

the mutant receptor contained a mixture of small and large particles (Fig. 4A, center and right), with the smaller particles resembling those found in the wild-type receptor samples. The heights and radii of a number of receptor particles were determined, as indicated in Fig. 4B. Particle radius was measured at half the maximal height to compensate for the tendency of AFM to overestimate this parameter because of the geometry of the tip (Barrera et al., 2005). Particle dimensions were used to calculate molecular volumes via the equation  $V_m = (\pi h/6)(3r^2 + h^2)$ , where  $h$  is the particle height and  $r$  is the radius (Schneider et al., 1998). The frequency distribution of the calculated molecular volumes for the wild-type P2X<sub>6</sub> subunit is shown in Fig. 4C. The distribution was fitted well by a single Gaussian function. The frequency distribution peaked at a molecular volume of  $121 \pm 6 \text{ nm}^3$  ( $n = 344$ ). The predicted volume for a single P2X<sub>6</sub> subunit of molecular mass 52 kDa is  $125 \text{ nm}^3$ , very close to the measured value. These results confirm our previous conclusion that the wild-type receptor subunits do not form stable oligomers. The presence of two types of particles in the S2K mutant receptor samples (above) was reflected in the frequency distribution of molecular volumes (Fig. 4D), which had two peaks at  $120 \pm 3 \text{ nm}^3$  ( $n = 215$ ) and  $340 \pm 20 \text{ nm}^3$  ( $n = 158$ ), indicating that approximately 42% of the mutant P2X<sub>6</sub> receptor particles are homotrimers.

In further experiments, S2K mutant P2X<sub>6</sub> receptors were imaged after incubation with a mouse monoclonal antibody that recognized the C-terminal His<sub>6</sub> tag. The sample contained various structures, including large and small particles. The smaller particles represent either monomeric receptor subunits or immunoglobulin G molecules, which are approximately the same size. The larger particles are homotrimers of the S2K mutant P2X<sub>6</sub> receptor subunits, as discussed above. Some of the large particles had one (arrows), two (arrowheads), or occasionally three (data not shown)

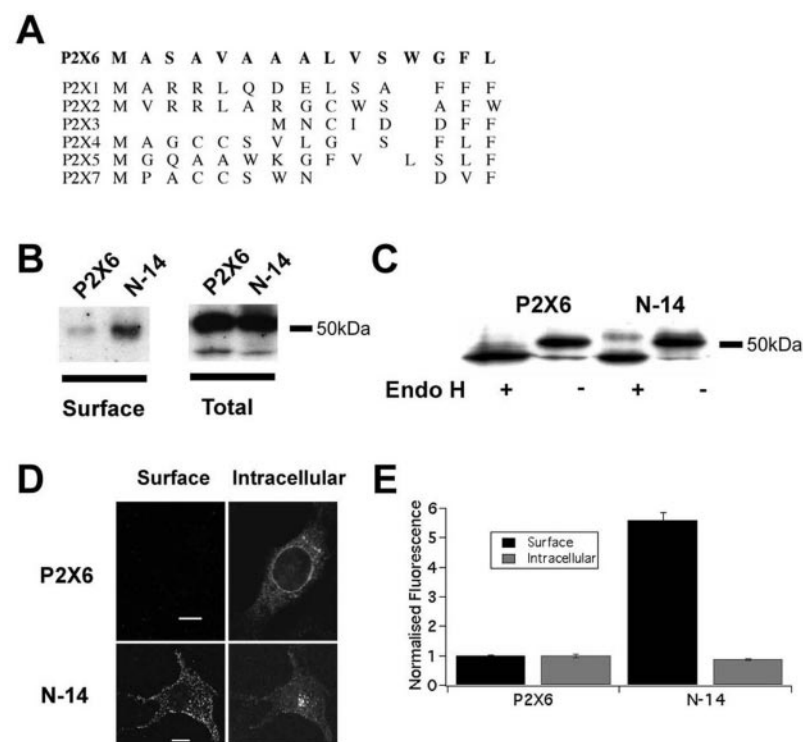


**Fig. 2.** The uncharged N-terminal region of the P2X<sub>6</sub> subunit promotes ER retention. **A**, sequence alignment of the first 14 N-terminal residues of the P2X<sub>6</sub> subunit with the corresponding regions of the other rat P2X subunits. **B**, comparison of surface expression of wild-type P2X<sub>6</sub> subunit and N-14 mutant, determined by biotinylation. **C**, Endo H digestion of crude detergent extracts of NRK cells expressing wild-type or N-14 P2X<sub>6</sub> subunits. **D**, confocal images of surface and intracellular distribution of wild-type or N-14 P2X<sub>6</sub> subunit. **E**, comparison of normalized surface/intracellular fluorescence given by wild-type and N-14 P2X<sub>6</sub> subunits ( $n = 73$ –76 cells for each condition).

smaller particles attached (Fig. 5A). These structures are likely to be receptors that have been liganded by one, two, or three antibody molecules. The various structures in the im-

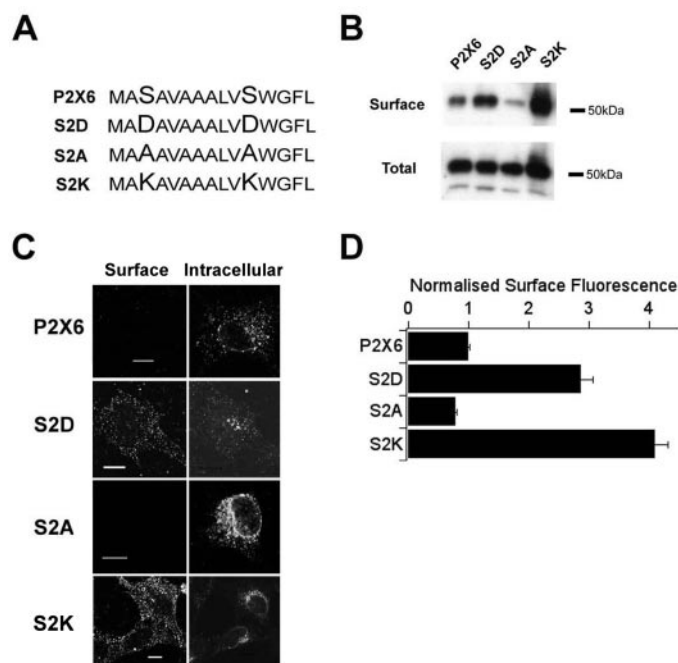


**Fig. 3.** ER retention is correlated with hydrophobicity at positions 3 and 11. **A**, comparison of the first 14 amino acids of the wild-type P2X<sub>6</sub> subunit with those of the three P2X<sub>6</sub> serine mutants. **B**, comparison of surface expression of the wild-type P2X<sub>6</sub> subunit and the serine mutants determined by biotinylation ( $n = 3$  blots). **C**, confocal images of surface/intracellular distribution of the wild-type P2X<sub>6</sub> subunit and the S2D, S2A, and S2K mutants. **D**, comparison of normalized surface and intracellular fluorescence given by the wild-type P2X<sub>6</sub> subunit or the S2D, S2A, and S2K mutants ( $n = 70$ – $103$  cells for each condition).

ages were analyzed, and their relative frequencies were determined. When the receptor was incubated with the anti-His<sub>6</sub> antibody, of 694 larger particles analyzed, 71.0% were unliganded; 20.2% had one antibody bound; and 7.8% had two bound antibodies. A very small proportion of the receptors (1.0%) had three bound antibodies. When receptors were imaged alone, only a small percentage of the larger particles (2.5% of a total of 162) seemed to be associated with bound particles. These presumably represent structures that happened to attach to the mica alongside receptors. These data indicate that the vast majority of the binding events observed with the anti-His<sub>6</sub> antibody represent specific receptor-antibody interactions.

Figure 5B shows a gallery of images of receptors with zero, one, and two bound antibodies. In the case of doubly liganded receptors, the angles between the pairs of bound antibodies are also shown. These angles were calculated for each complex by joining the height peaks of the antibody particles to the height peak of the receptor particle. The angles between the pairs of antibodies were determined and used to construct the frequency distribution shown in Fig. 5C. The mean of the distribution is  $124 \pm 4^\circ$  ( $n = 54$ ), very close to the value of  $120^\circ$  predicted for a trimeric receptor.

We conclude from these results that the introduction of charged residues within the P2X<sub>6</sub> N terminus promotes ER export and plasma membrane expression by promoting the formation of stable homotrimers. To test whether these N-terminal mutants produced functional ATP-gated channels, patch-clamp recordings were made from transfected HEK 293 cells, and ATP (10–1000  $\mu$ M) was applied locally by picrospritzer. All experiments were carried out on mutant P2X<sub>6</sub> subunits that did not contain the FLAG epitope. At a holding potential of  $-60$  mV, neither the deletion mutant nor

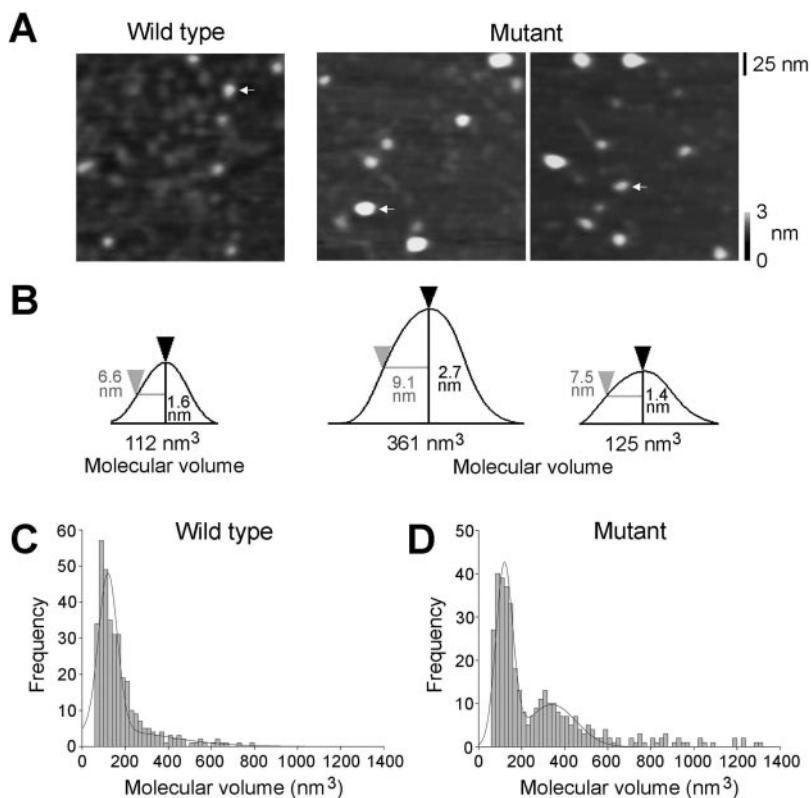


**Fig. 4.** AFM imaging of wild-type and S2K P2X<sub>6</sub> receptors. **A**, low-magnification images of wild-type (left) or S2K mutant (center and right) P2X<sub>6</sub> receptors bound to mica. A shade-height scale is shown at the bottom right. **B**, sections through the particles indicated by arrows in **A**. The procedures for measurement of the height of the particles (black) and their radii at half height (gray) are illustrated, and the calculated molecular volumes are shown for each particle. **C** and **D**, frequency distributions of the molecular volumes of the wild-type (**C**) and S2K (**D**) P2X<sub>6</sub> samples. The curves indicate the functions that were fitted to the data. The peak of the distribution in **C** corresponds to a molecular volume of  $121 \pm 6$  nm<sup>3</sup> ( $n = 344$ ), and the peaks in the distribution in **D** correspond to molecular volumes of  $120 \pm 3$  nm<sup>3</sup> ( $n = 215$ ) and  $340 \pm 20$  nm<sup>3</sup> ( $n = 158$ ).



the point mutants showed any response to ATP, whereas large inward currents were recorded from HEK 293 cells expressing P2X<sub>4</sub> (results not shown).

**The N-Terminal Region of the P2X<sub>6</sub> Subunit Enhances the ER Retention of P2X<sub>2</sub> but Does Not Prevent the Assembly of Functional Homomeric Receptors.** To test whether the hydrophobic N-terminal region of P2X<sub>6</sub> was sufficient to disrupt the assembly and export of P2X<sub>2</sub> receptors, we made a chimeric subunit in which this 14-amino acid region was substituted for the first half of the P2X<sub>2</sub> N terminus ([6N14] P2X<sub>2</sub>). For wild-type P2X<sub>2</sub>, the total protein ran as two bands on an immunoblot (70 and 64 kDa), with the higher molecular mass band being the predominant form at the surface. In contrast, for the chimera, the total protein ran at the lower molecular mass, with only a small proportion being fully glycosylated (Fig. 6A). Both the wild-type P2X<sub>2</sub> subunit and the chimera appeared at the surface, and after incubation with the cross-linking reagent DSS, both ran as a higher molecular mass complex, consistent with the formation of a trimer or higher molecular mass assembly (Fig. 6B). In addition, the chimeric receptor and the wild-type P2X<sub>2</sub> receptor were functional, with inward currents in response to 100  $\mu$ M ATP being significantly larger for the chimera than for the wild-type P2X<sub>2</sub> receptor (Fig. 6, E and F). However, when surface and intracellular expression was quantified by immunolabeling, there was a 2-fold decrease in surface stain-

ing and an increase in intracellular immunofluorescence for the chimera compared with the wild-type receptor (Fig. 6, C and D). Hence, the substitution of the distal N terminus of P2X<sub>6</sub> for the equivalent region of P2X<sub>2</sub> was not sufficient to prevent the formation of homotrimeric complexes but did promote ER retention.

## Discussion

We have shown that the P2X<sub>6</sub> subunit, when expressed individually, remains predominantly in monomeric form, in contrast to the P2X<sub>2</sub> subunit, which exists predominantly as trimers. The results presented here show that a double point mutation within the N terminus of P2X<sub>6</sub> is sufficient to promote the formation of homotrimers. The S2K mutation produced a shift in the distribution of receptor particles from monomers to a mixture of monomers and trimers. Thus, homoassembly was promoted, although it was still less efficient than the assembly of P2X<sub>2</sub> trimers. At the same time, there was an increase in complex glycosylation and delivery of P2X<sub>6</sub> to the plasma membrane. This effect was not criti-

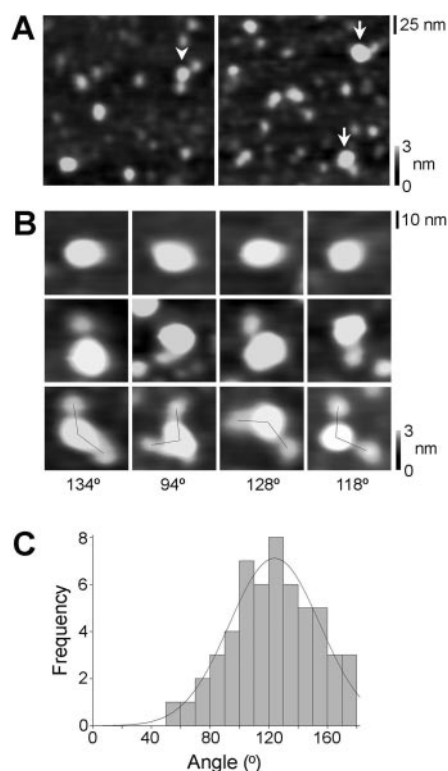


**Fig. 5.** AFM imaging of complexes between S2K P2X<sub>6</sub> homotrimers and anti-His<sub>6</sub> antibodies. A, images of receptor-antibody complexes. Receptors liganded by one antibody are indicated by arrows; a receptor liganded by two antibodies is indicated by arrowheads. A shade height scale is shown at the bottom right. B, gallery of zoomed images of receptors that are either unliganded (top) or liganded by one (middle) or two antibodies (bottom). The angles between the two bound antibodies at the bottom are shown. A shade height scale is shown at the bottom right. C, frequency distribution of angles between antibodies for 54 doubly liganded receptors. The curve indicates the Gaussian function that was fitted to the data. The mean ( $\pm$  S.E.M.) of the distribution is  $124 \pm 4^\circ$ .

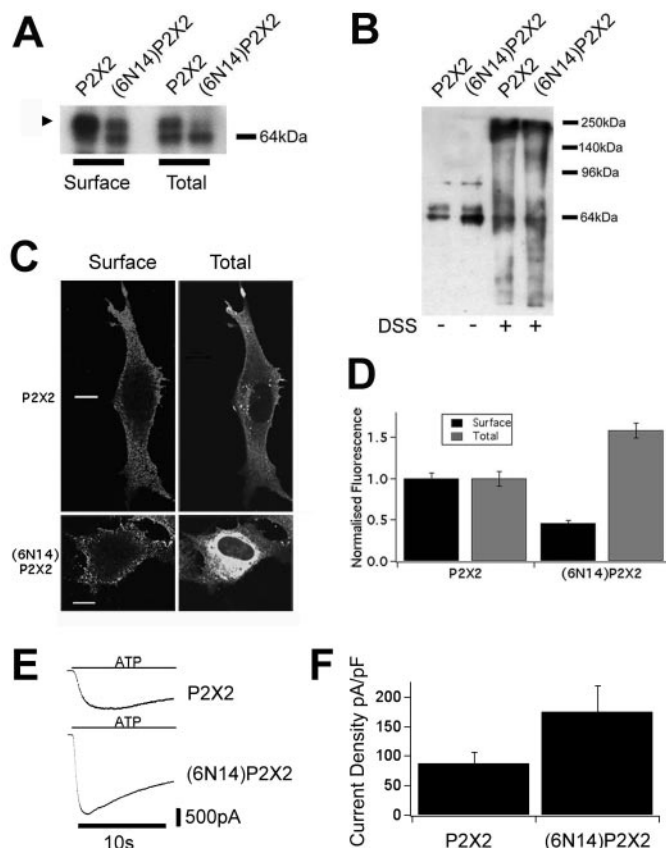


**Fig. 6.** The N-terminal region of the P2X<sub>6</sub> subunit is not sufficient to prevent coassembly and ER export of P2X<sub>2</sub> subunits. A, surface expression of wild-type P2X<sub>2</sub> and (6N14) P2X<sub>2</sub> subunits, assayed by biotinylation. The arrowhead indicates where the fully glycosylated P2X<sub>2</sub> is expected to run at 70 kDa. B, cross-linking of P2X<sub>2</sub> or (6N14) P2X<sub>6</sub> subunits by DSS. The position of molecular markers is shown on the right. The P2X<sub>2</sub> subunit was detected using an anti-P2X<sub>2</sub> polyclonal antibody. C, confocal images comparing surface and total distribution of P2X<sub>2</sub> subunits and (6N14) P2X<sub>2</sub> chimeras. D, comparison of normalized surface and intracellular fluorescence of cells expressing either P2X<sub>2</sub> or (6N14) P2X<sub>2</sub> subunits. E, whole-cell patch-clamp recordings from HEK 293 cells expressing either P2X<sub>2</sub> or the (6N14) P2X<sub>2</sub> chimera. Inward currents were evoked by 10  $\mu$ M ATP at a holding potential of  $-60$  mV. F, current densities (mean  $\pm$  S.E.M.,  $n = 5$ ) for the two receptors.

cally dependent on the nature of the amino acid substitution: both negatively and positively charged residues enhanced trafficking along the secretory pathway, as did deletion of the distal N-terminal region. From this result, we conclude that the mutations disrupt an interaction that normally exerts an inhibitory effect on the formation of stable homomeric receptors. Substituting less polar alanines, however, had the opposite effect, indicating a negative correlation between the hydrophobicity of the N-terminal region and the plasma membrane expression of the receptor. This in turn suggests that the distal N terminus of P2X<sub>6</sub> engages in either an intra- or an intermolecular hydrophobic interaction.

Although there is little sequence conservation within the N-terminal tail region between the various P2X subunits, P2X<sub>6</sub> is not unique in having a stretch of uncharged amino acids. For instance, P2X<sub>4</sub> has 13 uncharged amino acids at its N terminus compared with 15 for P2X<sub>6</sub> and yet is functional and is not retained in the ER (Bobanovic et al., 2002). Likewise, substitution of the N-terminal region of P2X<sub>6</sub> for the corresponding N-terminal region of the P2X<sub>2</sub> subunit was not sufficient to prevent the assembly and functional expression of the chimeric receptor, although it did enhance ER retention. Hence, it is likely that other parts of the P2X<sub>2</sub> and P2X<sub>4</sub> subunits either mask the N terminus or overcome the inhibitory effect by actively promoting the assembly process. This is consistent with the ability of P2X<sub>6</sub> to form functional heteromeric assemblies with both P2X<sub>2</sub> and P2X<sub>4</sub>.

There have been two previous reports that in a very small subset of transfected mammalian cells, the P2X<sub>6</sub> subunit is able to form functional homomeric receptors, although the functional properties reported for these receptors differs between the two studies (Collo et al., 1996; Jones et al., 2004). Our biotinylation data also indicated very low but detectable levels of the P2X<sub>6</sub> subunit at the cell surface. Furthermore, the extent of biotinylation was reduced by the serine-to-alanine mutations, suggesting that the biotinylated fraction did represent surface proteins and not simply the biotinylation of intracellular P2X<sub>6</sub> in permeabilized cells. We do not know whether this surface P2X<sub>6</sub> consists of unassembled subunits that have escaped the ER quality control machinery as a consequence of being overexpressed or correctly assembled trimers. We did not, however, record any responses to ATP from P2X<sub>6</sub>-transfected cells or observe any ATP-induced currents in cells transfected with the S2D, S2K, or N-14 mutants. It is possible that all of these mutations cause the homotrimeric receptor to be nonfunctional. However, the most likely explanation is that the homomeric P2X<sub>6</sub> complexes do not normally form functional ATP-gated cation channels and that the N terminal-dependent interaction is a mechanism to prevent the inappropriate assembly and plasma membrane expression of nonfunctional receptors.

Jones et al. (2004) showed that functional P2X<sub>6</sub> receptors had a considerably higher molecular mass than the nonfunctional protein: 70 compared with 60 kDa. Our data are inconsistent with these findings. The core-glycosylated form of the P2X<sub>6</sub> subunit ran on immunoblots at ~52 kDa, and its size was reduced to ~45 kDa after treatment with *N*-glycosidase F; furthermore, the increase in size upon association with P2X<sub>2</sub> or P2X<sub>4</sub> was very subtle (1–2 kDa). There was no indication of surface-biotinylated P2X<sub>6</sub> protein with a size close to 70 kDa in cells expressing either P2X<sub>2</sub>/P2X<sub>6</sub> or the P2X<sub>6</sub> mutant. It seems unlikely, therefore, that the func-

tional P2X<sub>6</sub> receptors reported previously represent heteromeric assemblies with endogenous P2X subunits. Our results do not, however, rule out the possibility that a minute fraction of transfected HEK 293 cells are able to process P2X<sub>6</sub> differently to make functional ATP receptors.

If P2X<sub>6</sub> is normally nonfunctional, what is its physiological role? Because the P2X<sub>6</sub> subunit can increase the calcium permeability of the P2X<sub>2</sub> receptor (Egan and Khakh, 2004) and change the pharmacology of both P2X<sub>2</sub> and P2X<sub>4</sub>, it might be “designed” to operate as a modulatory subunit rather than a receptor in its own right. This suggestion is substantiated by many reports of overlapping distributions of P2X<sub>6</sub> with P2X<sub>2</sub> and P2X<sub>4</sub> in both the central nervous system and the periphery (Collo et al., 1996; Soto et al., 1996; Rubio and Soto, 2001; Glass et al., 2002; Turner et al., 2003) and by the demonstration that P2X<sub>6</sub> is up-regulated under pathological conditions such as cancer and zinc deficiency (Urano et al., 1997; Nawa et al., 1999; Chu et al., 2003; Park et al., 2005). More recently, Liang et al. (2005) provided evidence of endogenous P2X<sub>4/6</sub> heteromers in a human bronchial epithelial cell line. Transfection of small interfering RNA fragments specific to P2X<sub>4</sub> or P2X<sub>6</sub> attenuated extracellular zinc- and ATP-induced Ca<sup>2+</sup> entry.

The involvement of the P2X<sub>6</sub> N terminus in receptor trafficking might be indirect, involving for instance the exposure of other hydrophobic regions or retention motifs within the unassembled subunit to chaperone proteins or COP I. One piece of evidence in support of a direct role in trafficking, however, is that the [6N14] P2X<sub>2</sub> chimeric receptor showed increased ER retention with no clear inhibition of subunit coassembly. There have been many studies investigating the mechanisms by which multimeric ion channels become retained within the ER. The most common retention motifs found within receptors are basic in nature; for example, twin lysine (KKXX) or arginine residues (RXR) (Teasdale and Jackson, 1996; Zerangue et al., 1999; Margeta-Mitrovic et al., 2000). Nevertheless, some uncharged motifs have been identified, including the CVLF motif within the C terminus of a splice-variant of the K<sup>+</sup> channel hSlo (Zarei et al., 2004). In addition, a hydrophobic retention sequence of 22 amino acids was identified in the C terminus of presenilin, a membrane protein that has cytosolic N and C termini. Similar to the region we have identified in P2X<sub>6</sub>, the presenilin sequence is mainly hydrophobic, with a few polar residues but no charged amino acids (Kaether et al., 2004).

One important difference between the majority of these receptors and the P2X<sub>6</sub> receptor is that when their retention motifs were mutated, only unassembled subunits were detected at the cell surface. In contrast, we have shown that as well as being able to exit the ER, the S2K mutant could also form homotrimers, albeit less efficiently than the P2X<sub>2</sub> subunit. This dual effect has also been shown for GluR2 subunits, which are also retained in the ER (Greger et al., 2002, 2003). The Q/R editing site in GluR2, previously believed to control just the calcium permeability of the receptor, is now known also to control receptor assembly. GluR2(R) was found to be largely unassembled in an intracellular pool, but editing to GluR2(Q) resulted in homotetramerization and elevated surface expression (Greger et al., 2003). GluR2(R) is the predominant subunit in vivo, and it was suggested that editing of the GluR2 subunit ensures that it is incorporated into  $\alpha$ -amino-3-hydroxy-5-methyl-4-isoxazolepropionic acid



receptors, albeit in a restricted fashion (Greger et al., 2003). ER retention of the P2X<sub>6</sub> subunit might then serve to prevent nonfunctional homomers from reaching the cell surface and/or to provide an intracellular pool of subunits ready to be incorporated into heteromeric receptors.

#### Acknowledgments

We thank Dr. L. Bobanovic for scientific input and experimental advice and S. Hayter for experimental assistance.

#### References

- Aschrafi A, Sadtler S, Niculescu C, Rettinger J, and Schmalzing G (2004) Trimeric architecture of homomeric P2X<sub>2</sub> and heteromeric P2X<sub>1+2</sub> receptor subtypes. *J Mol Biol* **342**:333–343.
- Barrera NP, Ormond SJ, Henderson RM, Murrell-Lagnado RD, and Edwardson JM (2005) Atomic force microscopy imaging demonstrates that P2X<sub>2</sub> receptors are trimers but that P2X<sub>6</sub> receptor subunits do not oligomerize. *J Biol Chem* **280**:10759–10765.
- Bobanovic LK, Royle SJ, and Murrell-Lagnado RD (2002) P2X receptor trafficking in neurons is subunit specific. *J Neurosci* **22**:4814–4824.
- Chu Y, Mouat MF, Coffield JA, Orlando R, and Grider A (2003) Expression of P2X<sub>6</sub>, a purinergic receptor subunit, is affected by dietary zinc deficiency in rat hippocampus. *Biol Trace Elem Res* **91**:77–87.
- Collo G, North RA, Kawashima E, Merlo-Pich E, Neidhart S, Surprenant A, and Buell G (1996) Cloning of P2X<sub>5</sub> and P2X<sub>6</sub> receptors and the distribution and properties of an extended family of ATP-gated ion channels. *J Neurosci* **16**:2495–2507.
- Deutsch C (2003) The birth of a channel. *Neuron* **40**:265–276.
- Durchschlag H and Zipper P (1997) Calculation of partial specific volumes and other volumetric properties of small molecules and polymers. *J Appl Crystallogr* **30**:803–807.
- Egan TM and Khakh BS (2004) Contribution of calcium ions to P2X channel responses. *J Neurosci* **24**:3413–3420.
- Ellgaard L and Helenius A (2003) Quality control in the endoplasmic reticulum. *Nat Rev Mol Cell Biol* **4**:181–191.
- Glass R, Loesch A, Bodin P, and Burnstock G (2002) P2X<sub>4</sub> and P2X<sub>6</sub> receptors associate with VE-cadherin in human endothelial cells. *Cell Mol Life Sci* **59**:870–881.
- Grant EH (1957) The dielectric method of estimating protein hydration. *Phys Med Biol* **2**:17–28.
- Greger IH, Khatri L, Kong X, and Ziff EB (2003) AMPA receptor tetramerization is mediated by Q/R editing. *Neuron* **40**:763–774.
- Greger IH, Khatri L, and Ziff EB (2002) RNA editing at arg607 controls AMPA receptor exit from the endoplasmic reticulum. *Neuron* **34**:759–772.
- Jones CA, Vial C, Sellers LA, Humphrey PP, Evans RJ, and Chessell IP (2004) Functional regulation of P2X<sub>6</sub> receptors by N-linked glycosylation: identification of a novel  $\alpha$ -methylene ATP-sensitive phenotype. *Mol Pharmacol* **65**:979–985.
- Kaether C, Capell A, Edbauer D, Winkler E, Novak B, Steiner H, and Haass C (2004) The presenilin C-terminus is required for ER-retention, nicastrin-binding and gamma-secretase activity. *EMBO (Eur Mol Biol Organ) J* **23**:4738–4748.
- King BF, Townsend-Nicholson A, Wildman SS, Thomas T, Spyer KM, and Burnstock G (2000) Coexpression of rat P2X<sub>2</sub> and P2X<sub>6</sub> subunits in *Xenopus* oocytes. *J Neurosci* **20**:4871–4877.
- Kukley M, Barden JA, Steinhäuser C, and Jabs R (2001) Distribution of P2X receptors on astrocytes in juvenile rat hippocampus. *Glia* **36**:11–21.
- Le KT, Villeneuve P, Ramjaun AR, McPherson PS, Beaudet A, and Seguela P (1998) Sensory presynaptic and widespread somatodendritic immunolocalization of central ionotropic P2X ATP receptors. *Neuroscience* **83**:177–190.
- Liang L, Zsembery A, and Schwiebert EM (2005) RNA interference targeted to multiple P2X receptor subtypes attenuates zinc-induced calcium entry. *Am J Physiol* **289**:C388–C396.
- Loesch A and Burnstock G (2001) Immunoreactivity to P2X<sub>6</sub> receptors in the rat hypothalamo-neurohypophyseal system: an ultrastructural study with extravidin and colloidal gold-silver labelling. *Neuroscience* **106**:621–631.
- Margeta-Mitrovic M, Jan YN, and Jan LY (2000) A trafficking checkpoint controls GABA<sub>B</sub> receptor heterodimerization. *Neuron* **27**:97–106.
- Maley F, Trimble RB, Tarentino AL, and Plummer TH Jr (1989) Characterization of glycoproteins and their associated oligosaccharides through the use of endoglycosidases. *Anal Biochem* **180**:195–204.
- Nawa G, Miyoshi Y, Yoshikawa H, Ochi T, and Nakamura Y (1999) Frequent loss of expression or aberrant alternative splicing of P2XM, a p53-inducible gene, in soft-tissue tumours. *Br J Cancer* **80**:1185–1189.
- Nicke A, Baumert HG, Rettinger J, Eichele A, Lambrecht G, Mutschler E, and Schmalzing G (1998) P2X<sub>1</sub> and P2X<sub>3</sub> receptors form stable trimers: a novel structural motif of ligand-gated ion channels. *EMBO (Eur Mol Biol Organ) J* **17**:3016–3028.
- North RA (1996) P2X receptors: a third major class of ligand-gated ion channels. *Ciba Found Symp* **198**:91–109.
- Park HC, Seong J, An JH, Kim J, Kim UJ, and Lee BW (2005) Alteration of cancer pain-related signals by radiation: proteomic analysis in an animal model with cancer bone invasion. *Int J Radiat Oncol Biol Phys* **61**:1523–1534.
- Rubio ME and Soto F (2001) Distinct localization of P2X receptors at excitatory postsynaptic specializations. *J Neurosci* **21**:641–653.
- Schneider SW, Larmer J, Henderson RM, and Oberleithner H (1998) Molecular weights of individual proteins correlate with molecular volumes measured by atomic force microscopy. *Pflueg Arch Eur J Physiol* **435**:362–367.
- Seguela P, Haghighi A, Sghomorian JJ, and Cooper E (1996) A novel neuronal P<sub>2X</sub> ATP receptor ion channel with widespread distribution in the brain. *J Neurosci* **16**:448–455.
- Soto F, Garcia-Guzman M, Karschin C, and Stuhmer W (1996) Cloning and tissue distribution of a novel P2X receptor from rat brain. *Biochem Biophys Res Commun* **223**:456–460.
- Teasdale RD and Jackson MR (1996) Signal-mediated sorting of membrane proteins between the endoplasmic reticulum and the Golgi apparatus. *Annu Rev Cell Dev Biol* **12**:27–54.
- Torres GE, Egan TM, and Voigt MM (1998) Topological analysis of the ATP-gated ionotropic P2X<sub>2</sub> receptor subunit. *FEBS Lett* **425**:19–23.
- Torres GE, Egan TM, and Voigt MM (1999a) Hetero-oligomeric assembly of P2X receptor subunits. Specificities exist with regard to possible partners. *J Biol Chem* **274**:6653–6659.
- Torres GE, Egan TM, and Voigt MM (1999b) Identification of a domain involved in ATP gated ionotropic receptor subunit assembly. *J Biol Chem* **274**:22359–22365.
- Turner CM, Vonend O, Chan C, Burnstock G, and Unwin RJ (2003) The pattern of distribution of selected ATP-sensitive P2 receptor subtypes in normal rat kidney: an immunohistological study. *Cells Tissues Organs* **175**:105–117.
- Urano T, Nishimori H, Han H, Furuhashi T, Kimura Y, Nakamura Y, and Tokino T (1997) Cloning of P2XM, a novel human P2X receptor gene regulated by p53. *Cancer Res* **57**:3281–3287.
- Vulchanova L, Arvidsson U, Riedl M, Wang J, Buell G, Surprenant A, North RA, and Elde R (1996) Differential distribution of two ATP-gated channels (P2X receptors) determined by immunocytochemistry. *Proc Natl Acad Sci USA* **93**:8063–8067.
- Zarei MM, Eghbali M, Alioua A, Song M, Knaus HG, Stefani E, and Toro L (2004) An endoplasmic reticulum trafficking signal prevents surface expression of a voltage- and Ca<sup>2+</sup>-activated K<sup>+</sup> channel splice variant. *Proc Natl Acad Sci USA* **101**:10072–10077.
- Zerangue N, Schwappach B, Jan YN, and Jan LY (1999) A new ER trafficking signal regulates the subunit stoichiometry of plasma membrane K(ATP) channels. *Neuron* **22**:537–548.

**Address correspondence to:** Dr. Ruth Murrell-Lagnado, Department of Pharmacology, University of Cambridge, Tennis Court Road, Cambridge CB2 1PD, United Kingdom. E-mail: rdm1003@cam.ac.uk